applied sciences

MDPI

Article

Adaptive Neural Trajectory Tracking Control for Synchronous Generators in Interconnected Power Systems

Ruben Tapia-Olvera [1], Francisco Beltran-Carbajal [2,*] and Antonio Valderrabano-Gonzalez [3]

[1] Departamento de Energía Eléctrica, Universidad Nacional Autónoma de México, Mexico City 04510, Mexico
[2] Departamento de Energía, Unidad Azcapotzalco, Universidad Autónoma Metropolitana, Av. San Pablo No. 180, Col. Reynosa Tamaulipas, Mexico City 02200, Mexico
[3] Facultad de Ingeniería, Universidad Panamericana, Álvaro del Portillo 49, Zapopan 45010, Mexico
* Correspondence: fbeltran@azc.uam.mx

Abstract: The synchronous generator is one of the most important active components in current electric power systems. New control methods should be designed to guarantee an efficient dynamic performance of the synchronous generator in strongly interconnected nonlinear power systems over a wide range of variable operating conditions. In this context, active suppression capability for different uncertainties and external disturbances represents a current trend in the development of new control design methodologies. In this paper, a new adaptive neural control scheme based on differential flatness with a modified structure including B-spline Neural Networks for transient stabilization and tracking of power-angle reference profiles for synchronous generators in interconnected electric power systems is introduced. These features are attained due to the advantages extracted of these two approaches: (a) a control design stage based on a power system model by differential flatness and (b) an adaptive performance using a correct design of B-spline Neural Networks, minimizing parameter dependency. The effectiveness of the proposed algorithm is demonstrated by simulation results in two test systems: single machine infinite bus and an interconnected power system. Transient stability and robust power-angle reference profile tracking are both verified.

Keywords: synchronous generator; interconnected power systems; vibration suppression; Artificial Neural Networks; trajectory tracking control

check for updates

Citation: Tapia-Olvera, R.; Beltran-Carbajal, F.; Valderrabano-Gonzalez, A. Adaptive Neural Trajectory Tracking Control for Synchronous Generators in Interconnected Power Systems. *Appl. Sci.* **2023**, *13*, 561. https://doi.org/10.3390/app13010561

Academic Editor: Andreas Sumper

Received: 1 December 2022
Revised: 15 December 2022
Accepted: 21 December 2022
Published: 31 December 2022

Copyright: © 2022 by the authors. Licensee MDPI, Basel, Switzerland. This article is an open access article distributed under the terms and conditions of the Creative Commons Attribution (CC BY) license (https://creativecommons.org/licenses/by/4.0/).

1. Introduction

Electric energy demand is increasing everyday; thus, electric power engineers must pay special attention to the new grid topologies, including emerging technologies focused on the generation tasks. In this context, transient stability analysis is a critical stage in any power system where the Synchronous Generator (SG) is a key component for the dynamic performance [1].

Due to the power system's complexity, it is important to delimit the phenomena under analysis considering the time scales, where these dynamics are presented. The problem of power system stability is known by the power system community regarding the classification discussed in [1–3]. In [3], the definition and classification of power system stability, including the new relevant dynamic phenomena, have been revised. Transient stability as a part of rotor angle stability is recognized as a desirable study in power systems. A review of some important aspects on the damping of power system oscillations is presented in [4]. Important strategies are reviewed and compared among them to define some criteria to evaluate their performance in the face of the challenges of modern electric power systems. Robust control strategies are an important alternative for generation units [5].

High-performance control design of multi-input and multi-output nonlinear interconnected electric power systems demands accurate mathematical models and knowledge of the physical parameters [6,7], especially when a large operational range is needed.

Important control strategies for the synchronous generator in power systems, covering linear, nonlinear and adaptive approaches have been proposed. However, the power system might confront complex phenomena that could cause failure on the control algorithms if these phenomena are not considered as included in the design stage. In that sense, nonlinear controllers for stabilization and synchronization of interconnected synchronous generators emerge as an alternative solution.

In [8], a Proportional-Integral-Derivative (PID) linear scheme, combined with a Non-Linear Threshold Accepting Algorithm (NLTA), is used to design a robust strategy that combines an Automatic Voltage Regulator and a Load Frequency Control (AVR-LFC) for a multi-area power system. The results after several trials show the ability of the NLTA to adjust its performance under different operating scenarios and improve the transient responses. On the other hand, a fractional-order sliding mode controller for the stability of a multimachine power system is proposed in [9]. This controller is used to make the power system stable in a fixed time, independent of the initial operating conditions. The proposal to regulate the excitation of the synchronous generators improves the transient stability of the power system by reducing the chattering phenomena and ensuring the power system stabilization in an upper bound time. This enhances the dynamic performance of the power system. In [10], a control strategy for the interconnected power system is proposed. The design procedure requires three stages—observer, fractional sliding mode surface and controller—but the procedure requires the definition of several considerations to guarantee the expected performance.

Moreover, model uncertainty and unknown external dynamic disturbances represent challenging issues that should be considered in the robust and efficient planned motion tracking control design problem for complex practical nonlinear dynamic systems. In this sense, a control approach based on the backstepping control design methodology and adaptive Neural Networks for a wheelchair upper-limb exoskeleton robot system is introduced in [11]. Furthermore, in [12] sliding modes and adaptive Neural Networks have been properly combined for developing a fixed-time position tracking control method for a wheelchair upper-limb exoskeleton robot system subjected to exogenous disturbances. In [13], the uncertainty of the nonlinear dynamic model, the time-varying external disturbances and the friction resistance of the n-link robotic manipulator are integrated into the uncertainty of the system as well. An adaptive robust term is used to compensate for this uncertainty. A reward function combining a Gaussian function and the Euclidean distance is designed for efficient and stable learning of the reinforcement learning agent. In this method, the parameters of the controller are adjusted and optimized in real time. The results show that the reward value obtained increases gradually with the increase in learning times, so, for slow processes, this method might be useful. By comparison, a controller design based on Multilayer Perceptron Neural Network (MLPNN) is developed in [14]. The proposed strategy can be very effective in control of the distributed multi-agent synchronous generator system. An online backpropagation algorithm is applied on MLPNN to distinguish the uncertainties of the SG model and update and regulate the weights of MLPNN adaptively based on the principles of consensus error. The controller can be applied as a learning scheme for estimation of the multi-agent system states, especially where there is no prior knowledge about the dynamics of leader/follower agent systems. However, the selection of parameters for the Neural Networks can substantially affect the accuracy of the proposed controller. Similarly, Ref. [15] presents a PID controller optimization procedure under constraints of model uncertainties and noise measurement, for a synchronous generator automatic voltage regulator with good results, but a plant model of the exciter is needed. This could be a drawback of the proposal due to the fact that data of the exciter are often unavailable. Some schemes for the stabilization and synchronization of SG are focused to having an efficient use of computational resources as detailed in [16]. There, an adaptive control based on the motion programmed trajectory is used for synchronous generators. In the procedure, it requires the proper choice of the reference

model. Moreover, it is mentioned that the strategy shows a promising level of robustness against disturbances. The strategy is recommended for SG from small to medium size.

In [17], an H-infinity control for the SG is proposed. The state vector is feedback in the control scheme and the solution of the Riccati equation is carried out. The technique is tested in a three machine power system. The control eliminates the disturbances, making the generators converge to the desirable setpoints, but big jumps are observed when transitions are presented. In contrast, Ref. [18] proposes an adaptive controller to damp oscillations and to enhance the Single Machine Infinite Bus (SMIB) stability. An adaptive linear Neural Network is employed as online model identification to mimic online the SMIB output. The coefficients of the SMIB model are adjusted online and then they are employed for estimating the parameters of the controllers. This method can be used in systems with large perturbation and parameter modifications to reduce oscillation and tuned time. In the same way, Ref. [19] presents an extended linear quadratic regulator designed for linear time-invariant systems in the presence of exogenous inputs with a novel feedback control structure. It can be used in model-based and model-free versions with net cost minimization by using dynamic programming. Disturbances in the system can be considered as exogenous inputs; however, the methodology is still not validated with large scale power systems.

The sensitivity analysis with respect to frequency variations, fault in tie-line, power flow and output reaction of dissimilar generators after instant load fluctuation in the planned structure in terms of dispersion of wind is discussed in [20]. Here, several controllers are compared in delay time, rise time, peak overshoot time and settling time. The power system consistent operation requires constant balancing of source and load. The proposal includes moth flame optimizer variants to mitigate the frequency constraint issue. In addition, the interconnection and damping assignment method is presented in [21] where the SG model is represented as a Port Controlled Hamiltonian system. The applicability of that proposed scheme is illustrated by the simulation results for efficient reference voltage tracking and attenuation of electromechanical oscillations when large disturbances are presented.

The electric power system is one of the most complex systems that engineers have created. Moreover, its relation demand/generation is changing continuously. It has to respond in a fast way when adverse events (some of them severe) take place and ensure its good performance with the integration of new components [22]. However, dealing with this wide range of variables in the control design stage is not always possible. Thus, adaptive control algorithms could overcome this drawback by updating the control response to the new circumstances of the power system and for a particular steady state condition. These dynamic requirements must be largely guaranteed by auxiliary control elements of SG with a suitable regulation strategy. Therefore, new control strategies must interact in a positive way with the current controllers with less dependency of model and parameters of components in the power system [23].

The automatic voltage regulator in SG plays a fundamental role in the power system dynamic performance. However, the model dependency of the control strategies could degrade the performance of the system due to the continuous changes in electrical grid operation. This dependency could be minimized with an adaptive performance included in the regulation strategy when large scale power systems are evaluated. With the proposed strategy it is possible to include uncertainties in the formulation, avoiding higher complexity by using a scheme based on B-spline Neural Networks.

There are several ways to model an SG. The appropriate model selection depends on the time-scales and phenomena under study [2,3]. For small system analysis, detailed models are often used [1]. Considering the transient response, a simplified model is commonly used, which includes the electromechanical variables along with the internal voltage. This model presents a compromise between the description of the dynamics of interest and a reduction in the computational complexity to attain a solution for large scale power systems.

This paper deals with the problem of transient stabilization and tracking of the reference profile of the power-angle for synchronous generators in interconnected electric power systems. A new adaptive neural stabilization strategy within the context of a reference trajectory tracking problem in interconnected power systems is proposed. In the presented approach, differential flatness and B-spline Neural Networks are synergically combined to compensate significant parametric uncertainty and reduce dependency in detailed nonlinear mathematical models of synchronous generators in interconnected power systems. Traditionally, two main approaches have been used in this sense, the first, based on the mathematical model and the last, based on measurements. Moreover, the problem significantly increases when more synchronous machines are included in the formulation, as occurs in real power systems. With our proposed strategy, the advantages of both approaches are extracted. First a systematic design procedure for the controller of each SG is obtained where the number of included machines is not a restriction and then simultaneous fine tuning is developed for each controller without additional requirements in design stage or knowledge of current steady state condition. The last task is carried out with the B-spline Neural Network scheme, which replies for changes in the system to attain the desired dynamic performance, without the need of the system model. Moreover, since the steady state of the power system is continuously changing due to the load demand, the proposed strategy is a very suitable option for variable online operation.

In the present contribution, a nonlinear dynamic model of the synchronous generator in interconnected power systems is used to evaluate two electrical grid topologies: (i) single machine infinite bus; (ii) two interconnected power systems. This representation is then used to design a new robust adaptive neural trajectory-tracking control scheme, where dependency on detailed nonlinear dynamic models is considerably reduced. Robustness in the presented scheme is also attained with an adaptive performance by the inclusion of B-spline Neural Networks, which compute the best values of the control design parameters.

2. Materials and Methods

This section details the models and methodology used in the proposed strategy for the description of a synchronous generator and its interaction with the power system. Transient stabilization of the interconnected power system and robust tracking of power-angle reference profiles specified for the generators are both guaranteed by using a B-spline and a differential flatness-based adaptive trajectory tracking control scheme. Two different topologies are introduced with possibility to extend the strategy to systems with uncertainties involved.

2.1. Modelling of Synchronous Generators in Large Scale Power System

The analysis of the dynamic behavior of power systems is an important research topic, as it is considered a problem for secure system operation [2,3]. The system performance is continuously changing due to the connected loads and it is possible for it to present disturbances of diverse nature and duration. Thus, the operation of installed controllers is vital to update the required reference values and respond to disturbances.

Transient stability studies in the power system are recommended for proving the closed-loop stable nonlinear dynamic system operation under severe time-varying disturbances. In this sense, a nonlinear dynamic model of the synchronous generator can be used for design purposes of efficient reference trajectory tracking control. In this context, the well known transient model for a synchronous generator constitutes a very good alternative. Moreover, this nonlinear dynamic model can be extended to large scale power systems as follows [24].

$$\begin{aligned}\dot{\delta}_i &= \omega_i \\ \dot{\omega}_i &= (P_{m_i} - P_{e_i} - D_i\omega_i)\sigma_i \\ \dot{E}_i &= -a_i E_i + b_i \sum_{j=1, j\neq i}^{n_g} E_j Y_{ij} \cos(\delta_i - \delta_j + \theta_{ij}) + E_{fi} + u_i \end{aligned} \tag{1}$$

with

$$P_{e_i} = G_{ii}E_i^2 + E_i \sum_{j=1, j\neq i}^{n_g} E_j Y_{ij} \sin(\delta_i - \delta_j + \theta_{ij}), \quad i = 1, \ldots, n_g \tag{2}$$

where B_{Mii} is the susceptance and G_{ii} is the conductance, both from the reduced admittance matrix. Here, the subscript i is used to denote the *i-th* machine under analysis and n_g represents the number of synchronous generators in the electrical grid. In addition, δ_i is the power angle; ω_i is the speed deviation from synchronous velocity; D_i is the damping coefficient; $\sigma_i = \pi f / H_i$ with H_i as the inertia constant and f the grid nominal frequency; P_{m_i} is the mechanical input power, which could exhibit possible variations; P_{e_i} is the electric power; E_{fd} is the steady state value of the excitation voltage; thus, $E_f = \frac{E_{fd}}{T'_{d0_i}}$; u_i identifies the control input signal which defines the variation from steady state value of the automatic voltage regulator; Y_{ij} and θ_{ij} are the magnitude and the angle of the ij component of reduced admittance matrix of Y_{bus}, respectively,

$$Y_{ij} \triangleq \sqrt{G_{ij}^2 + B_{ij}^2}, \quad \theta_{ij} \triangleq arctan\frac{G_{ij}}{B_{ij}} \tag{3}$$

The values for a_i and b_i are determined by the generator parameters as

$$a_i \triangleq \frac{1}{T'_{d0_i}}[1 - B_{Mii}(x_{di} - x'_{di})], \quad b_i \triangleq \frac{x_{di} - x'_{di}}{T'_{d0_i}} \tag{4}$$

where T'_{d0_i} is the direct-axis transient time constant; x_{di} and x'_{di} are the direct-axis synchronous reactance and transient reactance, respectively.

The SG is represented by a simplified transient model. This representation considers an internal voltage source behind the direct axis transient reactance in series with the armature resistance. Thus, using the reduced admittance matrix, the dynamics of the power system can be evaluated considering the internal voltages.

The reduced admittance matrix is calculated after obtaining the power flow solution by applying the Kron reduction. Thus, all loads are determined by equivalent admittances to ground and are included in the bus admittance matrix. The power system dynamics is evaluated with this formulation, where only the generator internal nodes are used for each iteration utilizing the reduced admittance matrix of dimension $n_g \times n_g$.

2.2. Control Analysis for a Single Machine Infinite Bus System

In this subsection, the mathematical representation of a single machine infinite bus system is developed from Equation (1). A proposal for output feedback control for desired power-angle reference trajectory tracking based on differential flatness and Neural Networks is introduced.

2.2.1. Model of a SMIB Power System

In Figure 1, a typical representation of a machine connected to a large capacity power system equivalent (Single Machine Infinite Bus, SMIB) is presented. The power system and SG parameters are $H = 5; D = 0.0; x'_d = 0.2$ pu; $x_d = 1.6$ pu; $T'_{d0} = 6$ s, while for buses and lines in pu $\mathbf{V}_\infty = 1.0\angle 0^\circ; \mathbf{V}_t = 1.0\angle\theta_t; P_e = 0.8; x_l = 0.2; x_T = 0.2$ are considered.

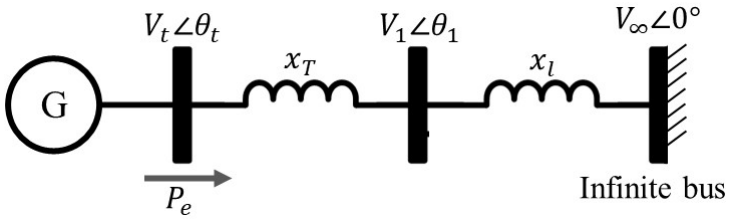


Figure 1. Single machine infinite bus power system.

From Equation (1), the synchronous machine model for the case of single machine infinite bus is described by

$$\begin{aligned}\dot{\delta} &= \omega \\ \dot{\omega} &= (P_m - P_e - D\omega)\sigma \\ \dot{E} &= -aE + bY\cos(\delta+\theta) + E_f + u\end{aligned} \tag{5}$$

where the subscript $i = 1$ has been excluded. Here, it is considered that $V_\infty = 1.0\angle 0°$, as depicted in Figure 1. The electric power injected by the generator is thus given by

$$P_e = GE^2 + EY\sin(\delta+\theta) \tag{6}$$

The power flow solution for this steady state condition defines the angle of the terminal voltage as 18.6629°. With this information, the initial conditions are determined; thus, $E_{f0} = 1.3931$ pu; $E_0 = 1.0387$ pu; $\delta_0 = 27.5241°$.

2.2.2. A Trajectory Tracking Approach for SMIB

Without loss of generality, a single machine infinite bus power system is first considered in this section. A new output feedback adaptive neural control strategy based on differential flatness for both transient stabilization and robust tracking of desired power-angle reference profiles for a synchronous generator in interconnected power systems is proposed. Trajectory planning considers that transient stabilization of the system at a specified equilibrium (operation) point in the state space should be firstly performed. Next, the power system should be efficiently transferred to another desired operation condition by following a desired smooth reference profile into the designed safe operational region of the power system.

The controlled nonlinear dynamic system model (5) exhibits the structural property of differential flatness. That is, state and control variables can be parameterized in terms of a so-called flat output and a finite number of its time derivatives [25,26]. In fact, the power angle $y = \delta$ constitutes a flat output. From the time derivatives up to the third order of the flat output y, the differential parametrization of the system variables results in

$$\begin{aligned}\delta &= y \\ \omega &= \dot{y} \\ E &= f(y,\dot{y},\ddot{y}) \\ u &= \frac{1}{\gamma}\Big[\dddot{y} + \gamma aE - \gamma bY\cos(y+\theta) - \gamma E_f + \sigma YE\dot{y}\cos(y+\theta) \\ &\quad + \sigma D\ddot{y} - \sigma\dot{P}_m\Big]\end{aligned} \tag{7}$$

with control input gain γ given by

$$\gamma = -\sigma Y\sin(y+\theta) - 2\sigma GE \tag{8}$$

Hence, the flat output dynamics can be described with the following nonlinear differential equation:

$$\dddot{y} + \gamma aE - \gamma bY\cos(y+\theta) - \gamma E_f + \sigma YE\dot{y}\cos(y+\theta) + \sigma D\ddot{y} = \gamma u - \sigma\dot{P}_m \tag{9}$$

An output feedback tracking controller for power-angle reference profiles $y^*(t) = \delta^*(t)$ can be then synthesized as

$$u = \frac{1}{\gamma}\left[\dddot{y}^* - \beta_3(\ddot{y} - \ddot{y}^*) - \beta_2(\dot{y} - \dot{y}^*) - \beta_1(y - y^*) - \beta_0\int_0^t (y - y^*)dt - \xi\right] \tag{10}$$

with

$$\begin{aligned}\xi =& \gamma\left[-aE + bY\cos(y+\theta) + E_f\right] - \sigma YE\dot{y}\cos(y+\theta)\\ &- \sigma D\ddot{y} + \sigma\dot{P}_m\end{aligned} \tag{11}$$

In the present study, power-angle reference trajectories $y^*(t)$ to perform a smooth transference of the power system from an operating condition to another are described via Bézier curves [27]. The time derivatives of planned reference trajectories are then described via closed form mathematical expressions. Differentiation with respect to time of output signals can be implemented as well [28]. The integral reconstruction approach of time derivatives of output signals constitutes another alternative to be considered in the control design problem [29].

Implementation of the controller (10) into the controlled power system yields the closed-loop tracking error dynamics, $e_\delta = y - y^*$,

$$e_\delta^{(4)} + \beta_3 e_\delta^{(3)} + \beta_2\ddot{e}_\delta + \beta_1\dot{e}_\delta + \beta_0 e_\delta = 0 \tag{12}$$

Therefore, asymptotic tracking of the reference trajectory $y^*(t) = \delta^*(t)$ can be guaranteed by selecting the control design parameters β_j, $j = 0, \ldots, 3$, so that the characteristic polynomial associated with Equation (12) is a Hurwitz polynomial. Then,

$$\lim_{t\to\infty} e_\delta = 0 \quad \Rightarrow \lim_{t\to\infty} y = y^*$$

In this context, the following family of stable polynomials can be used to compute the controller parameters β_j:

$$P_{CL}(s) = (s+p)^4 \tag{13}$$

with $p > 0$. Then, the parameters β_j, $j = 0, \ldots, 3$, can be algebraically calculated in terms of a positive constant p as follows

$$\begin{aligned}\beta_0 &= p^4\\ \beta_1 &= 4p^3\\ \beta_2 &= 6p^2\\ \beta_3 &= 4p\end{aligned} \tag{14}$$

Certainly, the differential flatness controller (10) stands as a very good alternative for the tasks of stabilization and tracking of desired power-angle reference profiles for operational scenarios where the system parameters and nonlinear dynamics are known accurately.

In the present contribution, an adaptive trajectory tracking control scheme based on B-spline Artificial Neural Networks and differential flatness for scenarios where uncertainty represents a relevant issue is proposed. In the presented control approach, the term $\xi(t)$ is considered like a bounded time-varying disturbance (uncertainty) signal into a small window of time to be directly compensated by the neural adaptive control action. Unmodelled dynamics, parametric uncertainty and exogenous perturbations affecting the

flat output could be lumped into this unknown disturbing signal as well. In this regard, authors have proved in previous works that active disturbance suppression capability can be achieved by adding integral tracking error compensation into control signals [30]. In contrast to other active disturbance rejection control design methods, the real-time disturbance estimation is not necessary in the presented neural approach. Thus, the differential flatness control scheme is simplified as follows

$$u = \frac{1}{\gamma}\left[\dddot{y}^* - \beta_3(t)(\ddot{y} - \ddot{y}^*) - \beta_2(t)(\dot{y} - \dot{y}^*) - \beta_1(t)(y - y^*) - \beta_0(t)\int_0^t (y - y^*)dt\right] \quad (15)$$

Now, from another robust control design perspective, control parameters β_j, $j = 0, \ldots, 3$ are considered to be adaptive and computed online using B-spline Artificial Neural Networks properly in accordance with the operating conditions specified for the electric power system as described in the next section. Moreover, to the best of our knowledge, in the present work it is shown that the introduced neural differential flatness control approach can be extended for multiple synchronous generators in interconnected power systems.

2.3. Adaptive Scheme Based on B-Spline Neural Networks

The control law given by Equation (10) requires the design parameters β_i, which in the present contribution are calculated in an adaptive way. Thus, the regulation strategy becomes Equation (15). However, to guarantee a correct performance of the algorithm, dynamic control gains $\beta_i(t)$ are considered. An important alternative to attain this adaptive performance is the use of a class of Neural Networks with an instantaneous learning rule, named B-spline Neural Networks (BSNN) [31]. The BSNN has a structure of a layer of inputs, an internal layer where basis functions must be defined in a correct way considering the main features of the input signals and an output layer. In this paper, the output of the BSNN is defined to dynamically calculate the value of $p(t)$ in Equation (14); thus,

$$p(t) = \mathbf{B}^T\mathbf{W} \quad (16)$$

where $\mathbf{B}$ is a column vector of basis function output and $\mathbf{W}$ is a column vector with an updating rule which ponders the contribution of each neuron depending on the input signal information (weighting vector), p is a scalar. These vectors are with the same size and it depends on the number of neurons in the internal layer which is defined in the offline training. Two main stages are required to use this adaptive configuration: (i) offline, where a correct BSNN structure is defined, and (ii) online, where the BSNN is included in the control law responding to important changes in the input error; the reader can review more details of these steps in [32] and references therein. Two main characteristics are searching by the use of this topology: (i) a friendly NN structure with high accuracy when it is implemented and (ii) the possibility of an instantaneous learning rule as a perspective of online and continuous learning.

The recurrence of updating depends on the presented changes of the selected input signals, in this paper, this input is defined by the error between the desired trajectory and the actual one, $e_\delta(t) = y - y^*$. Three neurons are used in the hidden layer and the basis functions are defined of third order and the knot vectors between the limits of ± 5 as the procedure shows in [32]. The initial values of the weighting vector are obtained in the offline training where a map of input/output data is used, representing the typical dynamic operation of the power system. The increment in the instantaneous learning rule is determined by [31],

$$\Delta\mathbf{W}(e_\delta) = -\frac{\eta\mathbf{B}(e_\delta)}{\|\mathbf{B}(e_\delta)\|^2}e_\delta \quad (17)$$

where $\|\cdot\|$ denotes the Euclidean norm and (e_δ) defines the dependency on the input signal, this feature helps the algorithm attain high accuracy dynamic performance. Additionally, η is called the learning rate, which results in acceptable performance if it is defined as ≤ 1.0;

after, in the offline step a fine tuning is carried out to reach the best learning performance. Thus, the weighting vector updates as $\mathbf{W}_{new} = \mathbf{W}_{old} + \Delta\mathbf{W}$. To improve the learning rule convergence, it is proposed to add a dead band considering the main characteristics of the input signal e_δ; in this case, it is defined as 1×10^{-4}. If the error is less than this value, the increment $\Delta\mathbf{W}$ is zero; thus, the previous value is preserved.

In this way, it is feasible to define online a dynamic value of β_i in Equation (15). In this case, $p(t)$ is determined via Equation (16); then, it is possible to calculate Equation (14). Accordingly, any perturbation to the synchronous generator is observed by the proposed algorithm updating the design parameters β_i in the control law and, in consequence, an adaptive performance is achieved. The problem of determining the correct values of β_i, Equation (14), is overcome with this proposal; moreover, the desired dynamic performance is extend to more demanding topologies of the electric power system with multiple controllers, as described in Section 2.4; under this configuration, a positive interaction between them is demanded.

The architecture of the B-spline Neural Network consists of three neurons. In cases in which B-spline functions are defined, univariates of third order are constructed over the knot vector of $\{-0.05, 0.35, 0.75, 1.15\}$, $\{-1.15, -0.75, -0.35, 0.5\}$ and $\{-0.65, -0.15, 0.45, 0.95\}$, respectively. It is considering that the input is normalized. A learning rate of 0.15 is used to guarantee fast learning and a convergence of the training rule.

2.4. Control Analysis of Interconnected Power Systems

The second system under analysis consists of two power systems interconnected by a tie line, as presented in Figure 2. Each equivalent generator represents a coherent group of generators. It is considered that this group of coherent generators have similar control systems; thus, they can be aggregated to a generator model with an equivalent exciter and regulation scheme as well [33]. In the middle of the transmission line, a load is connected by a transformer, which includes a new bus, V_L, Figure 2. For this case, the dynamic of the two synchronous generators must be included in the design stage.

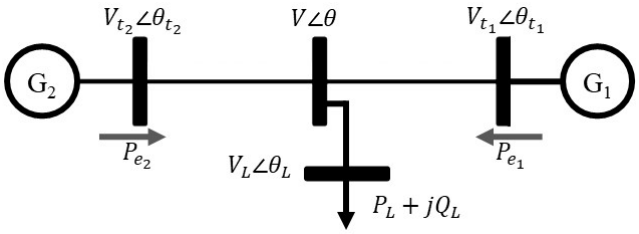


Figure 2. Interconnected power systems.

2.4.1. Model of Two Interconnected Systems

From Equation (1), the nonlinear dynamic model for this electrical grid topology results in

$$\begin{aligned}
\dot{\delta}_1 &= \omega_1 \\
\dot{\delta}_2 &= \omega_2 \\
\dot{\omega}_1 &= (P_{m_1} - P_{e_1} - D_1\omega_1)\sigma_1 \\
\dot{\omega}_2 &= (P_{m_2} - P_{e_2} - D_2\omega_2)\sigma_2 \\
\dot{E}_1 &= -a_1E_1 + b_1E_2Y_{12}\cos(\delta_1 - \delta_2 + \theta_{12}) + E_{f1} + u_1 \\
\dot{E}_2 &= -a_2E_2 + b_2E_1Y_{21}\cos(\delta_2 - \delta_1 + \theta_{21}) + E_{f2} + u_2
\end{aligned} \tag{18}$$

The electric power of each machine is defined by

$$\begin{aligned}
P_{e_1} &= G_{11}E_1^2 + E_1E_2Y_{12}\sin(\delta_1 - \delta_2 + \theta_{12}) \\
P_{e_2} &= G_{22}E_2^2 + E_2E_1Y_{21}\sin(\delta_2 - \delta_1 + \theta_{21})
\end{aligned} \tag{19}$$

where $\sigma_1 = \pi f / H_1$ and $\sigma_2 = \pi f / H_2$. Thus, Equation (18) describes the dynamic behavior of the electrical grid shown in Figure 2.

The line and machine data are shown in Table 1 and Table 2, respectively. Under this operation condition and system parameters, the constants calculated for the power system model (18) are presented in Table 3.

Table 1. Line data.

From	To	Resistance (pu)	Reactance (pu)	Tap Ratio
1	3	0	0.2	1.0
4	1	0	0.2	1.0
1	2	0	0.05	1.0

Table 2. Machine data.

Number	D	T'_{d0} [s]	x_d (pu)	x'_d (pu)	H [s]
1	0	6.0	1.6	0.2	5
2	0	6.0	1.55	0.19	4.5

Table 3. Constant values used in Equations (18) and (19).

Parameter	Value
G_{11}	0.3696
G_{22}	0.3888
$Y_{12} = Y_{21}$	1.1583
$\theta_{12} = \theta_{21}$	19.1032°
a_1	0.5010
a_2	0.4934
b_1	0.2333
b_2	0.2267

2.4.2. A Differential Flatness-Based Trajectory Tracking Approach

Synchronous generators for both multi-variable interconnected power systems exhibit the structural property of differential flatness. Power angles, $y_1 = \delta_1$ and $y_2 = \delta_2$, stand for flat outputs as well. State and control variables for this multi-output and multi-input nonlinear dynamic system with two generators can be also expressed in terms of the flat outputs as

$$\begin{aligned}
\delta_1 &= y_1 \\
\omega_1 &= \dot{y}_1 \\
E_1 &= f_1(y_1, \dot{y}_1, \ddot{y}_1, y_2, \dot{y}_2, \ddot{y}_2) \\
\delta_2 &= y_2 \\
\omega_2 &= \dot{y}_2 \\
E_2 &= f_2(y_1, \dot{y}_1, \ddot{y}_1, y_2, \dot{y}_2, \ddot{y}_2) \\
u_1 &= \frac{\dddot{y}_1 - \xi_1}{\gamma_1} \\
u_2 &= \frac{\dddot{y}_2 - \xi_2}{\gamma_2}
\end{aligned} \tag{20}$$

with control input gains given by

$$\begin{aligned}
\gamma_1 &= -\sigma_1 E_2 Y_{12} \sin(y_1 - y_2 + \theta_{12}) - 2\sigma_1 G_{11} E_1 \\
\gamma_2 &= -\sigma_2 E_1 Y_{21} \sin(y_2 - y_1 + \theta_{21}) - 2\sigma_2 G_{22} E_2
\end{aligned} \tag{21}$$

and

$$\begin{aligned}\xi_1 =& -\sigma_1 D_1 \dot{y}_1 - \gamma_1 a_1 E_1 + \gamma_1 b_1 E_2 Y_{12} \cos(y_1 - y_2 + \theta_{12}) + \gamma_1 E_{f1} \\ & - \sigma_1 E_1 \dot{E}_2 Y_{12} \sin(y_1 - y_2 + \theta_{12}) - \sigma_1 E_1 E_2 Y_{12} (\dot{y}_1 - \dot{y}_2) \cos(y_1 - y_2 + \theta_{12}) \\ & + \sigma_1 \dot{P}_{m1} \\ \xi_2 =& -\sigma_2 D_2 \dot{y}_2 - \gamma_2 a_2 E_2 + \gamma_2 b_2 E_1 Y_{21} \cos(y_2 - y_1 + \theta_{21}) + \gamma_2 E_{f2} \\ & - \sigma_2 E_1 E_2 Y_{21} (\dot{y}_2 - \dot{y}_1) \cos(y_2 - y_1 + \theta_{21}) - \sigma_2 E_2 \dot{E}_1 Y_{21} \sin(y_2 - y_1 + \theta_{21}) \\ & + \sigma_2 \dot{P}_{m2} \end{aligned} \tag{22}$$

Thus, dynamics of flat outputs can be described by the nonlinear differential equations

$$\begin{aligned}\dddot{y}_1 &= \xi_1 + \gamma_1 u_1 \\ \dddot{y}_2 &= \xi_2 + \gamma_2 u_2 \end{aligned} \tag{23}$$

Thence, for applications where detailed nonlinear mathematical models and knowledge of accurate system parameters are available, the following new differential flatness-based controllers for transient stabilization and tracking of desired power-angle profiles in the power system can then be derived as follows:

$$\begin{aligned}u_1 &= \frac{1}{\gamma_1}\left[\dddot{y}_1^* - \beta_{3,1}\ddot{e}_{\delta_1} - \beta_{2,1}\dot{e}_{\delta_1} - \beta_{1,1} e_{\delta_1} - \beta_{0,1}\int_0^t e_{\delta_1} dt - \xi_1\right] \\ u_2 &= \frac{1}{\gamma_2}\left[\dddot{y}_2^* - \beta_{3,2}\ddot{e}_{\delta_2} - \beta_{2,2}\dot{e}_{\delta_2} - \beta_{1,2} e_{\delta_2} - \beta_{0,2}\int_0^t e_{\delta_2} dt - \xi_2\right] \end{aligned} \tag{24}$$

where $e_{\delta_1} = y_1 - y_1^*$ and $e_{\delta_2} = y_2 - y_2^*$ denote the tracking errors.

Hence, closed-loop dynamics of power-angle reference profile tracking errors are governed by

$$\begin{aligned}e_{\delta_1}^{(4)} + \beta_{3,1}\dddot{e}_{\delta_1} + \beta_{2,1}\ddot{e}_{\delta_1} + \beta_{1,1}\dot{e}_{\delta_1} + \beta_{0,1} e_{\delta_1} = 0 \\ e_{\delta_2}^{(4)} + \beta_{3,2}\dddot{e}_{\delta_2} + \beta_{2,2}\ddot{e}_{\delta_2} + \beta_{1,2}\dot{e}_{\delta_2} + \beta_{0,1} e_{\delta_2} = 0 \end{aligned} \tag{25}$$

Thus, control design parameters $\beta_{j,i}$, $j = 1, \ldots, 3$, $i = 1, \ldots, 2$ should be selected properly to guarantee convergence of tracking errors e_i toward zero. Similarly, the following family of stable polynomials can be used to compute the control gains:

$$P_{CL,i}(s) = (s + p_i)^4 \tag{26}$$

with $p_i > 0$. Then,

$$\begin{aligned}\beta_{0,i} &= p_i^4 \\ \beta_{1,i} &= 4p_i^3 \\ \beta_{2,i} &= 6p_i^2 \\ \beta_{3,i} &= 4p_i \end{aligned} \tag{27}$$

2.5. Adaptive Neural Trajectory Tracking Control for Multiple SG in Interconnected Electric Power Systems

An adaptive trajectory tracking control scheme for multiple synchronous generators in interconnected power systems, based on differential flatness and B-spline Artificial Neural Networks, is proposed as follows

$$u_i = \frac{1}{\gamma_i}\left[\dddot{y}_i^* - \beta_{3,i}(t)\ddot{e}_{\delta_i} - \beta_{2,i}(t)\dot{e}_{\delta_i} - \beta_{1,i}(t) e_{\delta_i} - \beta_{0,i}(t)\int_0^t e_{\delta_i} dt\right], \quad i = 1, 2 \tag{28}$$

with tracking errors $e_{\delta_i} = \delta_i - \delta_i^*$. In the same way, the adaptive design parameters β_j, $j = 1, \ldots, 3$ are properly computed online using B-spline Artificial Neural Networks.

Notice that the present study provides insight for a future research extension of the presented adaptive neural robust control design perspective for other applications where dynamic models for synchronous generators exhibiting the differential flatness property, involving a higher number of nonlinear differential equations, are preferred to guarantee transient stability. This is for possible operating scenarios where flat output variables could be described by

$$y_i^{(n)} = \xi_i + \gamma_i u_i, \quad i = 1, 2, \ldots, n_g \tag{29}$$

with disturbances $\xi_i(t)$ being uniformly absolutely bounded:

$$\|\xi_i\|_\infty = \sup_{t \in [0,\infty)} |\xi_i(t)| = \lambda_i < \infty, \tag{30}$$

where λ_i stand for positive constants, the tracking control approach based on differential flatness and B-spline Neural Networks represents a very good alternative:

$$u_i = \frac{1}{\gamma_i}\left[y_i^{(n)*} - \beta_{n,i}(t)e_{\delta_i}^{(n-1)} - \cdots - \beta_{2,i}(t)\dot{e}_{\delta_i} - \beta_{1,i}(t)e_{\delta_i} - \beta_{0,i}(t)\int_0^t e_{\delta_i} dt\right] \tag{31}$$

Moreover, the adaptive control design parameters should be properly computed to guarantee closed-loop stability of the interconnected power system under study as described above.

3. Results and Discussion

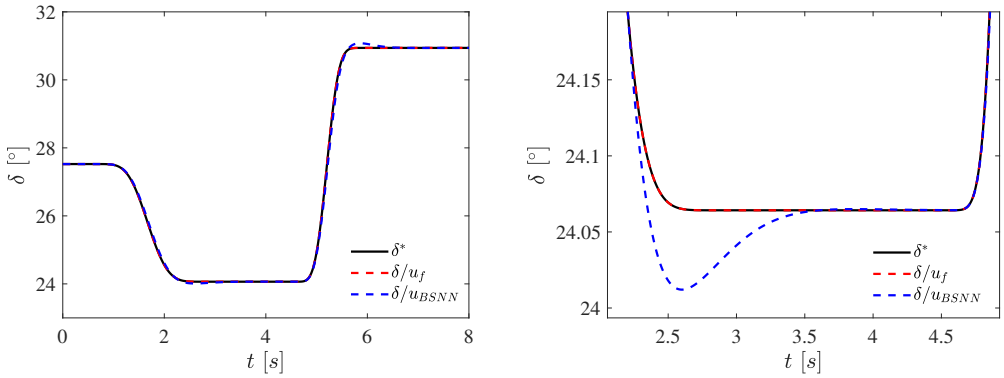
This section provides a description of the results of the strategy used in three different scenarios: a single machine connected to an infinite bus system, two interconnected power systems and finally considering this system with uncertainties.

3.1. Results for a Synchronous Generator with Adaptive Trajectory Tracking Scheme

The applicability of this proposal is also corroborated with time-domain simulations, where the nonlinear model of the SMIB power system given by Equation (5) is analyzed for trajectory tracking tasks. First, the used controller is defined by Equation (10), u_f in the time responses, where it was assumed that time-varying disturbances ξ are accurately known. Thas is, the control implementation considers that there is no dynamic uncertainty to be compensated. On the other hand, in the adaptive controller given by Equation (15), the knowledge of disturbances ξ becomes unnecessary. In this fashion, disturbances ξ are actively compensated by the proposed adaptive neural trajectory tracking control scheme. Now, the control parameters β_i are calculated by the adaptive scheme developed in Section 2.3, in time responses it is identified by u_{BSNN}. The model of SG described by Equations (1) and (2), with the proposed regulation strategy to operate the excitation system, were implemented in Matlab and solved numerically by the fourth-order Runge–Kutta method with a integration time-step of 1 ms. All simulations presented in this paper were carried out under this methodology. In Figures 3–6, it can be verified that the proposed adaptive trajectory tracking scheme has behavior very close to that obtained with the inclusion of time-varying disturbances ξ in the design stage, and the difference among them is marginal.

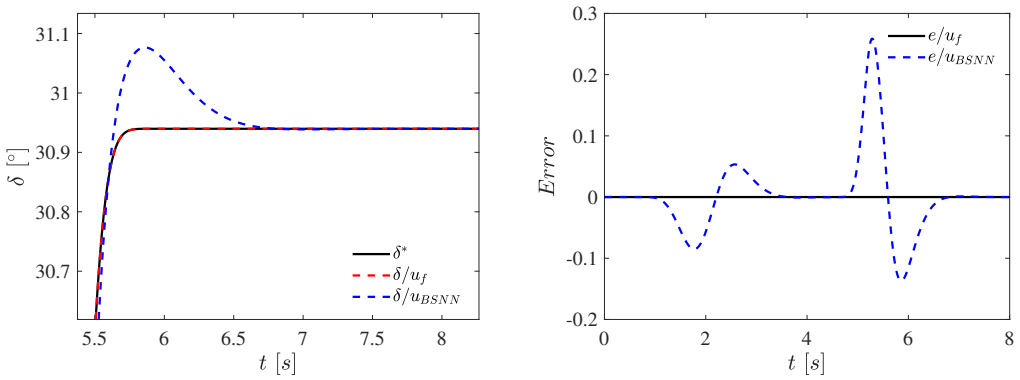
For this case, two changes in reference value of the load angle, δ^*, are presented at $t = 0.5$ s and $t = 4.5$ s, Figure 3. The first reference value is defined by the initial steady state condition of the power system, the second is $\delta^* = 24.0642°$ and the last one is $\delta^* = 30.9397°$. The width of the window where the change is exhibited is 1.5 s. The desired trajectory for load angle was specified to follow a smooth motion reference profile based on Bézier polynomials [34] with those values described above.

Figure 3 shows the behavior of the proposed adaptive scheme for tracking the desired trajectory. As can be observed in Figures 3b and 4a, the difference between both values is very close to zero with the most evident deviation when the current signal reaches the end value of the transition. These results confirm the expected performance of the proposed regulation scheme working together with the proposed adaptive algorithm, BSNN. The control signal calculated via Equations (10) and (15) are displayed in Figure 5a. With this behavior, the overshoot is almost eliminated and the performance of the tracking task is guaranteed for different values.



(**a**) (**b**)

Figure 3. Load angle response at generator of SMIB system: (**a**) δ; (**b**) zoom of δ when the reference value is decreased.

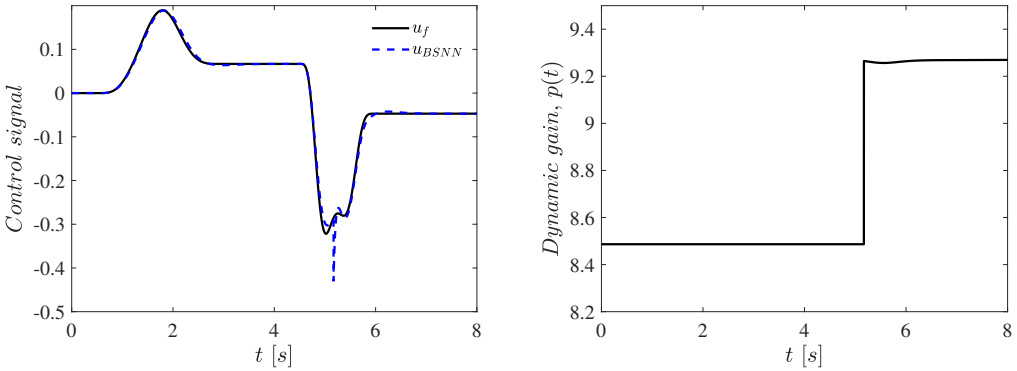


(**a**) (**b**)

Figure 4. SMIB system: (**a**) zoom of δ when the reference value is increased; (**b**) tracking error, $e = \delta - \delta^*$.

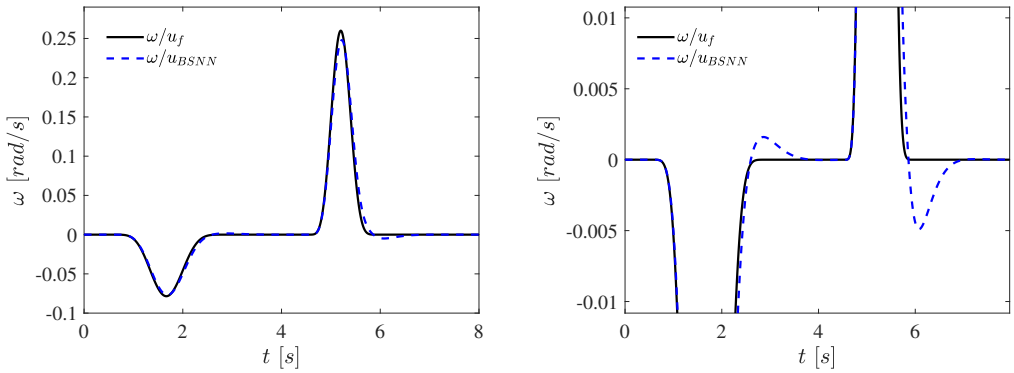
The difference of both regulation algorithms is marginal, as presented in Figure 5a. Thus, the difficulty of determining the correct values of the constant p is overcome with the adaptive scheme, which is responsible for decreasing the parameter dependency on the system model and has high accuracy for the task of trajectory tracking. The dynamic determination of this value permits one to attain the observed performance. The behavior of the BSNN structure is exhibited in the evolution of $p(t)$, Figure 5b.

The evolution of the speed deviation is in accordance with this performance. As depicted in Figure 6a,b, some visible variations are only exhibited when the main changes are presented. The dynamic behavior of all variables is very well bounded with high accuracy to follow the defined trajectory. The proposed adaptive strategy fulfills the primary task defined in the design stage.



(**a**) (**b**)

Figure 5. (**a**) Control signal u; (**b**) evolution of the parameter p used in the control scheme.



(**a**) (**b**)

Figure 6. Speed deviation: (**a**) ω; (**b**) zoom of ω in the main changes.

3.2. Results for an Equivalent of Interconnected Power Systems with Adaptive Trajectory Tracking Scheme

In this case, the connected load in the power system is 1.7 pu of real power and generators 1 and 2 feed 0.95 and 0.75 pu, respectively. The terminal voltage in each generator is $V_{t_1} = 1.021$ pu and $V_{t_2} = 0.98$ pu, respectively, resulting in a complex case with voltage magnitude in other nodes near the lower limit. The power flow solution for this condition is presented in Table 4. Based on this result, the initial conditions for the variables of the test power system are shown in Table 5.

Table 4. Power flow solution for a topology of Figure 2.

Bus	Voltage		P_{gen}	Q_{gen}	P_{load}	Q_{load}
	Magnitude (pu)	Angle (°)	(pu)	(pu)	(pu)	(pu)
1	0.9688	−11.0743	0	0	0	0
2	0.9648	−16.2918	0	0	1.7	0
3	1.0210	0	0.95	0.3585	0	0
4	0.9800	−1.9842	0.75	0.1144	0	0

Table 5. Initial conditions for the dynamic model.

Generator	δ_0 (°)	ω_0 (rad/s)	E_0 (pu)	E_{fd0} (pu)	P_m (pu)
1	9.6778	0	1.1070	1.8105	0.95
2	6.2713	0	1.0127	1.3193	0.75

In this case study, the desired references for each generator are changed. The presented scenarios are bounded by the permissible physical limits of the operation of electric power systems in terms of voltage magnitudes and powers. A more demanding operation condition is analyzed in this case considering an increment of real power in load node and including low values of voltage magnitude in some nodes. The set point at $t = 0.1$ s of δ_1^* is 11.4592° and at $t = 5.0$ s is 5.6723°. Moreover, in the case of generator 2, the set point starts with $\delta_2^* = 6.2713°$ and at $t = 2.5$ s it is changed to $\delta_2^* = 4.2972°$. The window of change is 1.5 s and it is calculated as in the SMIB case.

The dynamic evolution of the load angles of each generator using the proposed adaptive algorithm is shown in Figures 7 and 8. The trajectory tracking task is consistent with the results obtained for SMIB. Moreover, a zoom of these variables is presented in Figures 7b and 8b. The performance of the adaptive scheme is compared with one where all system information is available. Like in the case of SMIB, the proposed adaptive algorithm attains an expected behavior, with high accuracy for reference tracking. The errors between desired and actual power angle are presented in Figure 9a,b for generators 1 and 2, respectively.

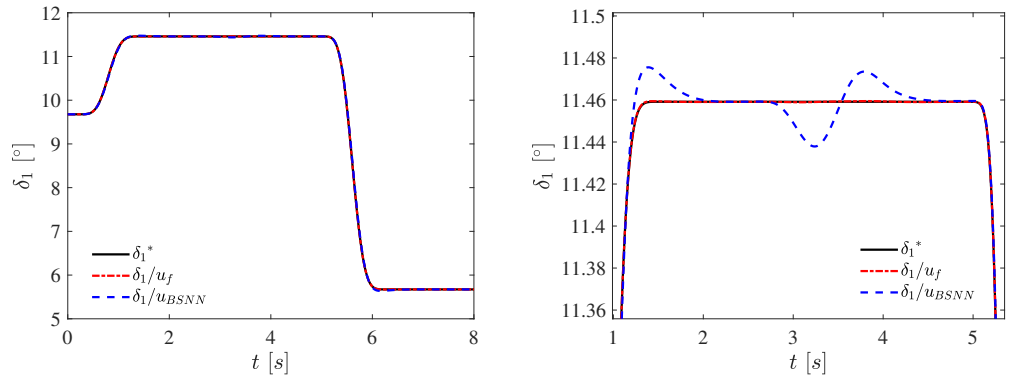


Figure 7. Load angle of generator 1 of two interconnected power systems: (**a**) δ_1; (**b**) zoom of δ_1.

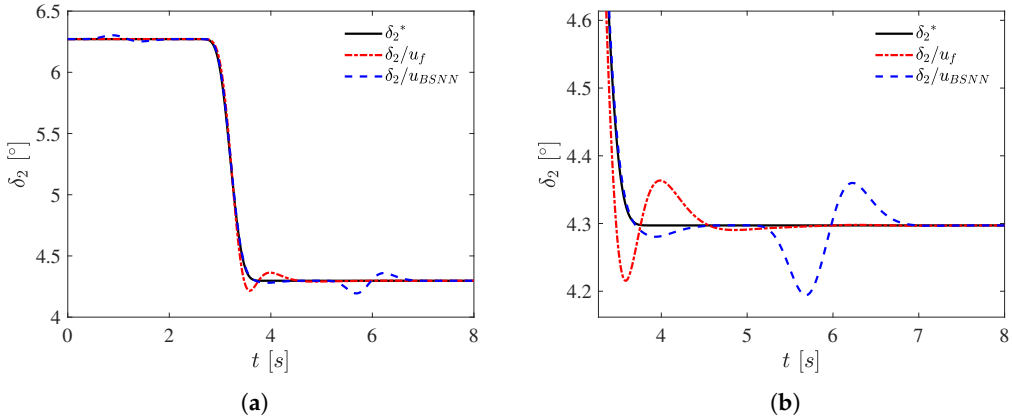
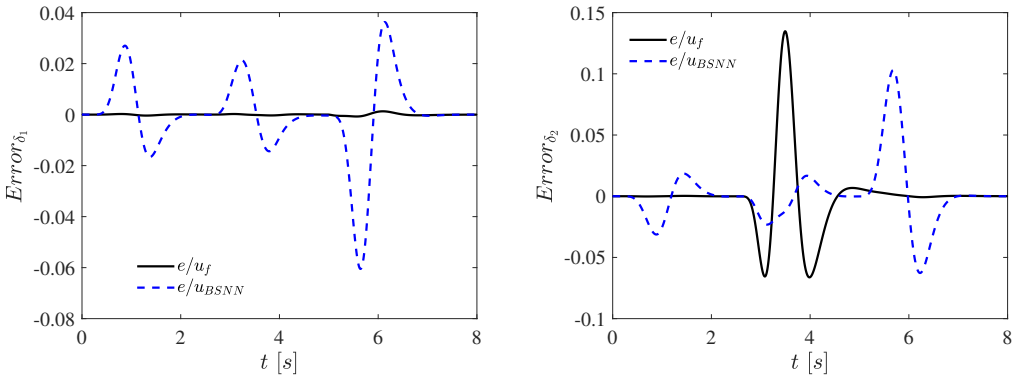


Figure 8. Load angle of generator 2 of two interconnected power systems: (**a**) δ_2; (**b**) zoom of δ_2.

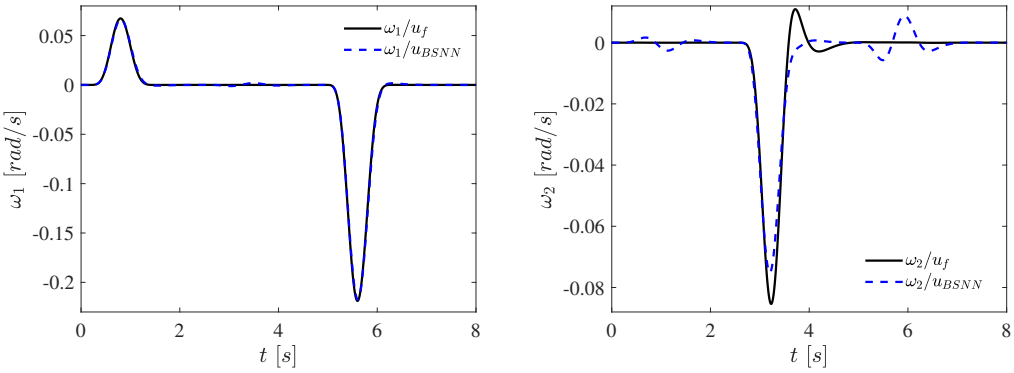
The deviation on the speed of each generator is presented in Figure 10. The larger variations are exhibited when changes in the reference value are presented. In steady state condition, the speed deviation returns to zero, which is accomplished with the proposed regulation scheme. The control input signals for each generator are presented in Figure 11, calculated with Equation (24) with $\xi = 0$, the BSNN scheme (u_{BSNN}) and the complete formulation (u_f). This behavior is reached due to the adaptive configuration introduced in this paper and the dynamic gain for each regulation algorithm presented in Figure 12.

Thus, the value of β_i is updating when the error between the reference and the actual load angle is increased.



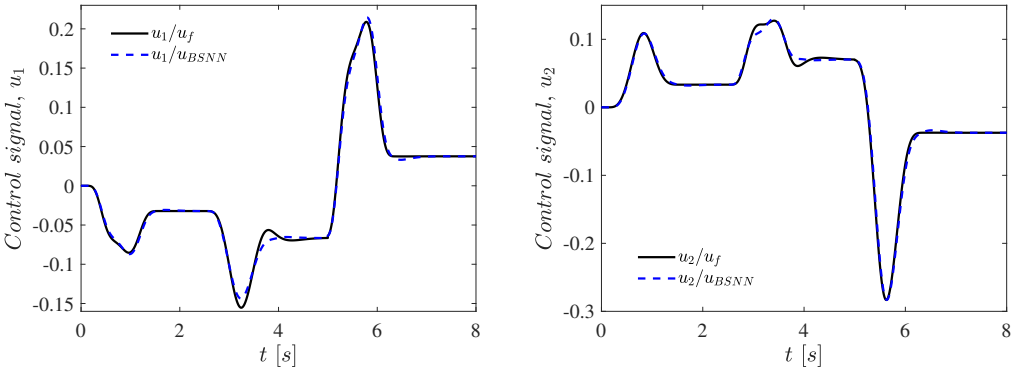
(**a**) (**b**)

Figure 9. Load angle reference trajectory tracking errors for (**a**) generator 1; (**b**) generator 2.



(**a**) (**b**)

Figure 10. Speed deviation of (**a**) generator 1; (**b**) generator 2.

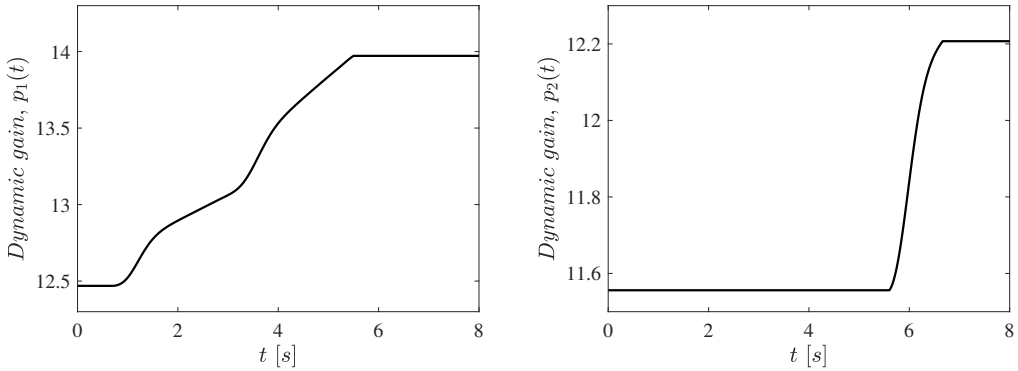


(**a**) (**b**)

Figure 11. Control signals: (**a**) u_1; (**b**) u_2.

3.3. Proposed Strategy Subjected to Uncertainties

The effectiveness of the proposed neural control strategy, subjected to uncertainties, is verified by simulation analysis. The power system of Figure 2 now has the line data of Table 6. The machine data of Table 2 now has damping coefficients of $D_1 = D_2 = 0.01$. The power flow solution is exhibited in Table 7 and the initial conditions in Table 8. The power system in this case includes active power losses in transmission lines, real and reactive load and coefficient damping different from zero.



(**a**) (**b**)

Figure 12. Evolution of the parameter p for the control scheme of each generator: (**a**) p_1; (**b**) p_2.

Table 6. Line data.

From	To	Resistance (pu)	Reactance (pu)	Tap Ratio
1	3	0.01	0.1	1.0
4	1	0.012	0.1	1.0
1	2	0.005	0.05	1.0

Table 7. Power flow solution.

Bus	Voltage		P_{gen}	Q_{gen}	P_{load}	Q_{load}
	Magnitude (pu)	Angle (°)	(pu)	(pu)	(pu)	(pu)
1	0.9784	−5.3769	0	0	0	0
2	0.9578	−10.5349	0	0	1.7	0.15
3	1.0000	0	0.9334	0.1653	0	0
4	1.0150	−0.9679	0.8000	0.3044	0	0

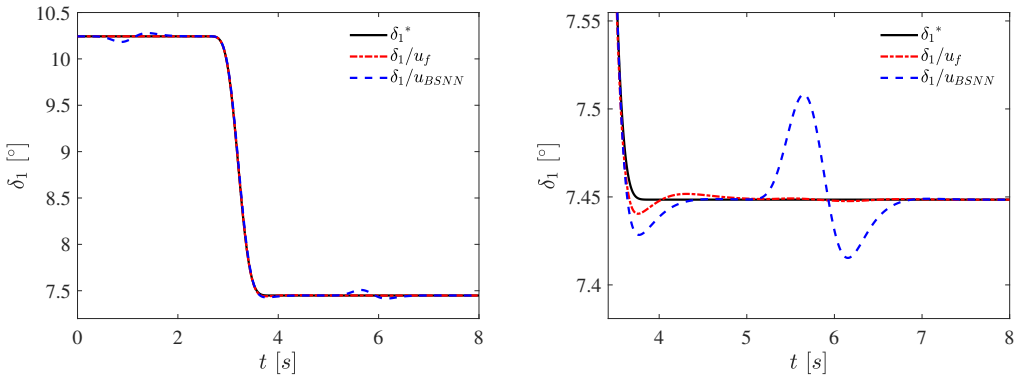
Table 8. Initial conditions for the third case study.

Generator	δ_0 (°)	ω_0 (rad/s)	E_0 (pu)	E_{fd0} (pu)	P_m (pu)
1	10.2431	0	1.0498	1.5099	0.9334
2	6.9847	0	1.0824	1.6347	0.8000

The same formulation is used and the control strategy is directly applied. At the beginning, it again solves the power flow formulation to then determine the initial condition. Thus, the reference tracking is demonstrated when the power system is subjected to parameter and variable changes. Figures 13 and 14 exhibit the capability of the proposed scheme to attain an excellent performance for reference tracking when variations in power system are presented. The speed in Figure 15 is in accordance with the results in previous analyzed cases, showing the most important deviation when the changes in reference value are presented. This performance is guaranteed by the correct determination of the control variable u, Figure 16. The evolution of the adaptive gains is presented in Figure 17. The comparison of the adaptive scheme performance with those obtained with the completed formulation of the control law is also included in the variables' evolution. This regulation strategy permits one to have a desirable transient response of the interest variables and a global positive impact in the other power system variables.

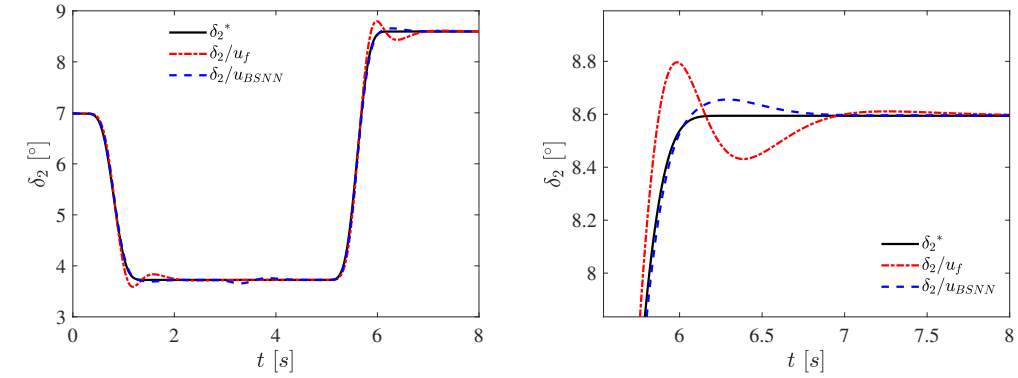
These results confirm the expected performance of the proposed adaptive regulation scheme, showing dynamic responses free of a large overshoot when changes are required

in the desired values for the power angle in each machine; also, the global variables' system behavior is in accordance with physical restrictions.



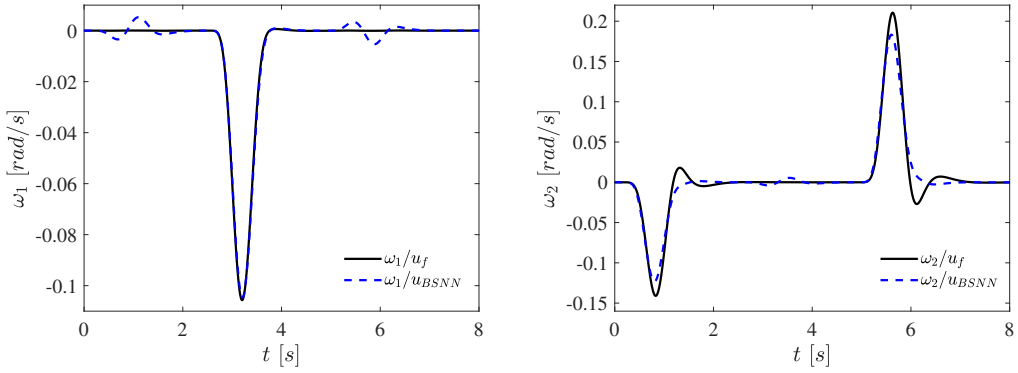
(**a**) (**b**)

Figure 13. Load angle of generator 1 of two interconnected power systems: (**a**) δ_1; (**b**) zoom of δ_1.



(**a**) (**b**)

Figure 14. Load angle of generator 2 of two interconnected power systems: (**a**) δ_2; (**b**) zoom of δ_2.

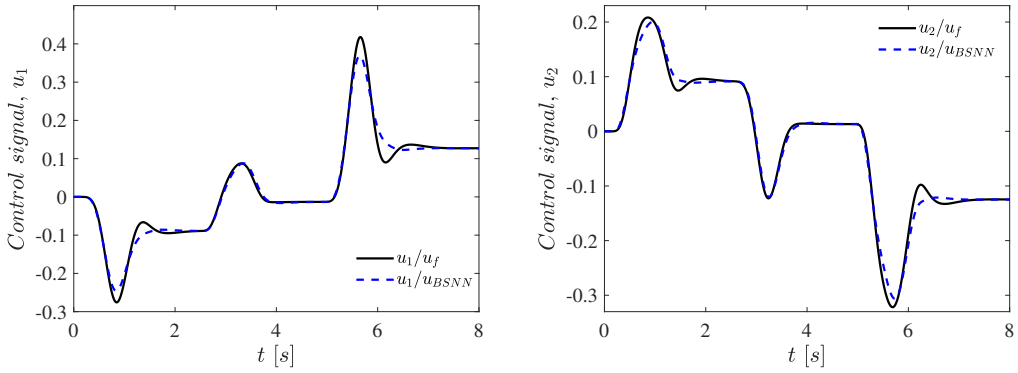


(**a**) (**b**)

Figure 15. Speed deviation of (**a**) generator 1; (**b**) generator 2.

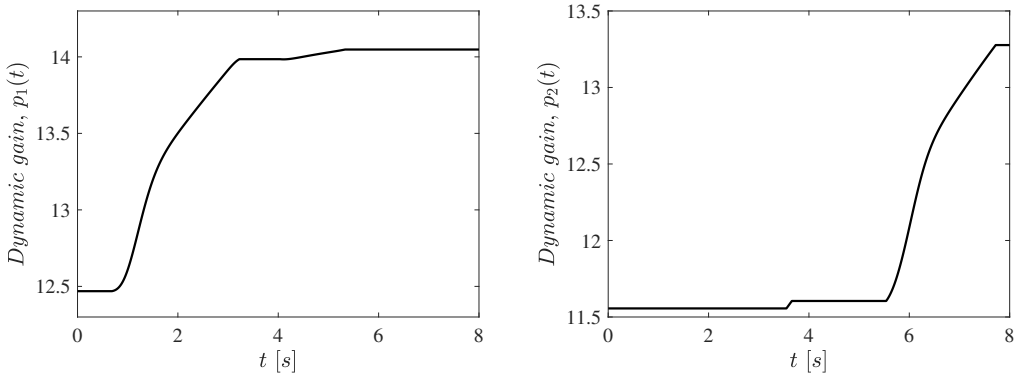
The growing and new topologies of electric power systems demand control strategies which could reduce the dependency of model, parameters and actual steady state condition. The results presented in this paper exhibit a desirable behavior combining two approaches, one based on the model and extending its applicability and robustness considering some measured variables. This is possible due to the proposed strategy with desirable features of online application with low computational demand. Thus, part of the uncertainty presented in the electrical grids could be compensated by continuous tuning of some critical controllers. Moreover, the evaluation of the proposed algorithm is carried out, including

important nonlinear phenomena presented in power systems which are considered in the used model.



(**a**) (**b**)

Figure 16. Control signals: (**a**) u_1; (**b**) u_2.



(**a**) (**b**)

Figure 17. Evolution of the parameter p for the control scheme of each generator: (**a**) p_1; (**b**) p_2.

Other approaches based either on model or measurements have demonstrated their applicability in systems. However, their performance is limited by the model utilized and the parameters of the system under test [22,23]. In addition, the complexity of the control design stage might substantially increase if modifications in grid topology are presented; moreover, the controller behavior could be degraded.

4. Conclusions

In this paper, it was demonstrated that the differential flatness property is observed in synchronous generators in interconnected power systems. Based on this feature, a robust control law can be defined and the applicability can be extended to scenarios with high uncertainty if it is synergically combined with B-spline Neural Networks. Thus, a satisfactory adaptive performance is reached and the parameter dependency is minimized. The proposed regulation algorithm based on the detail procedure presented in this paper was applied to interconnected power systems and it is possible to extend to other topologies of electric power systems. The obtained results in two topologies of electrical grids show the adaptability of the proposal for different power-angle reference profiles with bounded overshoot and very short settling time. Moreover, the transient responses of speed deviation of synchronous generators and all power system variables are very fast with bounded overshoot. Both transient stabilization and robust tracking of power-angle reference profiles for each synchronous generator are attained with this approach. Future research works will consider the robust tracking control design problem for Multi-Input Multi-Output (MIMO) large-scale interconnected nonlinear power systems using measurements of output signals only.

Author Contributions: Conceptualization, R.T.-O. and F.B.-C.; Data curation, R.T.-O.; Formal analysis, R.T.-O. and F.B.-C.; Investigation, R.T.-O., F.B.-C. and A.V.-G.; Methodology, R.T.-O. and F.B.-C.; Project administration, R.T.-O.; Resources, R.T.-O., F.B.-C. and A.V.-G.; Software, R.T.-O.; Supervision, R.T.-O. and F.B.-C.; Validation, R.T.-O.; Writing—original draft, R.T.-O., F.B.-C. and A.V.-G.; Writing—review & editing, R.T.-O., F.B.-C. and A.V.-G. All authors have read and agreed to the published version of the manuscript.

Funding: This research received no external funding.

Institutional Review Board Statement: Not applicable.

Informed Consent Statement: Not applicable.

Data Availability Statement: Not applicable.

Conflicts of Interest: The authors declare no conflict of interest.

References

1. Kundur, P. *Power System Stability and Control*, 1st ed.; McGraw-Hill Education: New York, NY, USA, 1994.
2. Kundur, P.; Paserba, J.; Ajjarapu, V.; Andersson, G.; Bose, A.; Canizares, C.; Hatziargyriou, N.; Hill, D.; Stankovic, A.; Taylor, C.; et al. Definition and classification of power system stability IEEE/CIGRE joint task force on stability terms and definitions. *IEEE Trans. Power Syst.* **2004**, *19*, 1387–1401.
3. Hatziargyriou, N.; Milanovic, J.; Rahmann, C.; Ajjarapu, V.; Canizares, C.; Erlich, I.; Hill, D.; Hiskens, I.; Kamwa, I.; Pal, B.; et al. Definition and Classification of Power System Stability—Revisited & Extended. *IEEE Trans. Power Syst.* **2021**, *36*, 3271–3281.
4. Rafique, Z.; Khalid, H.M.; Muyeen, S.; Kamwa, I. Bibliographic review on power system oscillations damping: An era of conventional grids and renewable energy integration. *Int. J. Electr. Power Energy Syst.* **2022**, *136*, 107556. [CrossRef]
5. Greidanus, M.D.R.; Heldwein, M.L. Model-Based Control Strategy to Reduce the Fault Current of a Gas Turbine Synchronous Generator under Short-Circuit in Isolated Networks. *Electr. Power Syst. Res.* **2022**, *204*, 107687. [CrossRef]
6. Wang, X.; Lv, Z.; Wang, R.; Hui, X. Optimization method and stability analysis of MMC grid-connect control system based on virtual synchronous generator technology. *Electr. Power Syst. Res.* **2020**, *182*, 106209. [CrossRef]
7. Elhaji, E.M.; Hatziadoniu, C.J. Damping tie-line power oscillations by modulation feedback of wind generators. *Electr. Power Syst. Res.* **2017**, *143*, 739–747. [CrossRef]
8. Nahas, N.; Abouheaf, M.; Sharaf, A.; Gueaieb, W. A Self-Adjusting Adaptive AVR-LFC Scheme for Synchronous Generators. *IEEE Trans. Power Syst.* **2019**, *34*, 5073–5075. [CrossRef]
9. Huang, S.; Xiong, L.; Wang, J.; Li, P.; Wang, Z.; Ma, M. Fixed-Time Fractional-Order Sliding Mode Controller for Multimachine Power Systems. *IEEE Trans. Power Syst.* **2021**, *36*, 2866–2876. [CrossRef]
10. Yang, F.; Shao, X.; Muyeen, S.; Li, D.; Lin, S.; Fang, C. Disturbance observer based fractional-order integral sliding mode frequency control strategy for interconnected power system. *IEEE Trans. Power Syst.* **2021**, *36*, 5922–5932. [CrossRef]
11. Aly, A.A.; Vu, M.T.; El-Sousy, F.F.; Hsia, K.H.; Alotaibi, A.; Mousa, G.; Le, D.N.; Mobayen, S. Adaptive Neural Network-Based Fixed-Time Tracking Controller for Disabilities Exoskeleton Wheelchair Robotic System. *Mathematics* **2022**, *10*, 3853. [CrossRef]
12. Aly, A.A.; Hsia, K.H.; El-Sousy, F.F.; Mobayen, S.; Alotaibi, A.; Mousa, G.; Le, D.N. Adaptive Neural Backstepping Control Approach for Tracker Design of Wheelchair Upper-Limb Exoskeleton Robot System. *Mathematics* **2022**, *10*, 4198. [CrossRef]
13. Lu, P.; Huang, W.; Xiao, J.; Zhou, F.; Hu, W. Adaptive Proportional Integral Robust Control of an Uncertain Robotic Manipulator Based on Deep Deterministic Policy Gradient. *Mathematics* **2021**, *9*, 2055. [CrossRef]
14. Sharifi, A.; Sharafian, A.; Ai, Q. Adaptive MLP Neural Network controller for consensus tracking of Multi-Agent systems with application to synchronous generators. *Expert Syst. Appl.* **2021**, *184*, 115460. [CrossRef]
15. Veinović, S.; Stojić, D.; Joksimović, D. Optimized four-parameter PID controller for AVR systems with respect to robustness. *Int. J. Electr. Power Energy Syst.* **2022**, *135*, 107529. [CrossRef]
16. Khrushchev, Y.V.; Khrushchev, I.Y.; Prokhorov, A.; Belyaev, N.; Vasiliev, A. Programmed trajectory motion control for synchronous generators. *Int. J. Electr. Power Energy Syst.* **2020**, *119*, 105884. [CrossRef]
17. Rigatos, G.; Siano, P.; Melkikh, A.; Zervos, N. A Nonlinear H-Infinity Control Approach to Stabilization of Distributed Synchronous Generators. *IEEE Syst. J.* **2018**, *12*, 2654–2663. [CrossRef]
18. Fawzy Rashwan, A.; Ahmed, M.; Mossa, M.R.; Baha-El-Din, A.M.; Alkhalaf, S.; Senjyu, T.; Hemeida, A.M. Explicit adaptive power system stabilizer design based an online identifier for single-machine infinite bus. *Ain Shams Eng. J.* **2022**, *13*, 101544. [CrossRef]
19. Mukherjee, S.; Bai, H.; Chakrabortty, A. Model-based and model-free designs for an extended continuous-time LQR with exogenous inputs. *Syst. Control Lett.* **2021**, *154*, 104983. [CrossRef]
20. Arora, K.; Kumar, A.; Kamboj, V.K.; Prashar, D.; Shrestha, B.; Joshi, G.P. Impact of Renewable Energy Sources into Multi Area Multi-Source Load Frequency Control of Interrelated Power System. *Mathematics* **2021**, *9*, 186. [CrossRef]
21. Jerković Štil, V.; Mehmedović, M. Interconnection and damping assignment automatic voltage regulator for synchronous generators. *Int. J. Electr. Power Energy Syst.* **2018**, *101*, 204–212. [CrossRef]

22. Sa'ed, J.A.; Favuzza, S.; Navarro Navia, M.A.; Zizzo, G. Virtual Synchronous Machine Control of RES Plants in Isolated Power Systems. *Appl. Sci.* **2022**, *12*, 5920. [CrossRef]
23. Haroon, S.I.A.; Qian, J.; Zeng, Y.; Zou, Y.; Tian, D. Extended State Observer Based-Backstepping Control for Virtual Synchronous Generator. *Electronics* **2022**, *11*, 2988. [CrossRef]
24. Ortega, R.; Galaz, M.; Astolfi, A.; Sun, Y.; Shen, T. Transient stabilization of multimachine power systems with nontrivial transfer conductances. *IEEE Trans. Autom. Control* **2005**, *50*, 60–75.
25. Fliess, M.; Lévine, J.; Martin, P.; Rouchon, P. Flatness and defect of non-linear systems: Introductory theory and examples. *Int. J. Control* **1995**, *61*, 1327–1361. [CrossRef]
26. Fliess, M.; Lévine, J.; Martin, P.; Ollivier, F.; Rouchon, P. Controlling nonlinear systems by flatness. In *Systems and Control in the Twenty-First Century*; Springer: New York, NY, USA, 1997; pp. 137–154.
27. Beltran-Carbajal, F.; Silva-Navarro, G. Generalized nonlinear stiffness identification on controlled mechanical vibrating systems. *Asian J. Control* **2019**, *21*, 1281–1292. [CrossRef]
28. Beltran-Carbajal, F.; Valderrabano-Gonzalez, A.; Rosas-Caro, J.; Favela-Contreras, A. An asymptotic differentiation approach of signals in velocity tracking control of DC motors. *Electr. Power Syst. Res.* **2015**, *122*, 218–223. [CrossRef]
29. Beltran-Carbajal, F.; Silva-Navarro, G. Output feedback dynamic control for trajectory tracking and vibration suppression. *Appl. Math. Model.* **2020**, *79*, 793–808. [CrossRef]
30. Beltran-Carbajal, F.; Tapia-Olvera, R.; Lopez-Garcia, I.; Valderrabano-Gonzalez, A.; Rosas-Caro, J.C.; Hernandez-Avila, J.L. Extended PI feedback tracking control for synchronous motors. *Int. J. Control. Autom. Syst.* **2019**, *17*, 1346–1358. [CrossRef]
31. Brown, M.; Harris, C. *Neurofuzzy Adaptive Modelling and Control*; Prentice Hall International (UK) Ltd.: Hemel Hempstead, UK, 1994.
32. Tapia-Olvera, R.; Beltran-Carbajal, F.; Valderrabano-Gonzalez, A.; Aguilar-Mejia, O. A Novel Methodology for Adaptive Coordination of Multiple Controllers in Electrical Grids. *Mathematics* **2021**, *9*, 1474. [CrossRef]
33. Wang, L.; Klein, M.; Yirga, S.; Kundur, P. Dynamic reduction of large power systems for stability studies. *IEEE Trans. Power Syst.* **1997**, *12*, 889–895. [CrossRef]
34. Beltran-Carbajal, F.; Tapia-Olvera, R.; Valderrabano-Gonzalez, A.; Yanez-Badillo, H.; Rosas-Caro, J.; Mayo-Maldonado, J. Closed-loop online harmonic vibration estimation in DC electric motor systems. *Appl. Math. Model.* **2021**, *94*, 460–481. [CrossRef]

Disclaimer/Publisher's Note: The statements, opinions and data contained in all publications are solely those of the individual author(s) and contributor(s) and not of MDPI and/or the editor(s). MDPI and/or the editor(s) disclaim responsibility for any injury to people or property resulting from any ideas, methods, instructions or products referred to in the content.